Am J Physiol Lung Cell Mol Physiol 288: L887–L893, 2005.
First published December 23, 2004; doi:10.1152/ajplung.00382.2004.

Pharmacokinetics of pulmonary manganese absorption: evidence for increased susceptibility to manganese loading in iron-deficient rats

Elizabeth Heilig,[1,2] Ramon Molina,[1] Thomas Donaghey,[1] Joseph D. Brain,[1] and Marianne Wessling-Resnick[2]

Departments of [1]Environmental Health and [2]Genetics and Complex Diseases, Harvard School of Public Health, Boston, Massachusetts

Submitted 12 October 2004; accepted in final form 22 December 2004

Heilig, Elizabeth, Ramon Molina, Thomas Donaghey, Joseph D. Brain, and Marianne Wessling-Resnick. Pharmacokinetics of pulmonary manganese absorption: evidence for increased susceptibility to manganese loading in iron-deficient rats. *Am J Physiol Lung Cell Mol Physiol* 288: L887–L893, 2005. First published December 23, 2004; doi:10.1152/ajplung.00382.2004.—High levels of airborne manganese can be neurotoxic, yet little is known about absorption of this metal via the lungs. Intestinal manganese uptake is upregulated by iron deficiency and is thought to be mediated by divalent metal transporter 1 (DMT1), an iron-regulated factor known to play a role in dietary iron absorption. To better characterize metal absorption from the lungs to the blood and test whether iron deficiency may modify this process, the pharmacokinetics of pulmonary manganese and iron absorption by control and iron-deficient rats were compared. Levels of DMT1 expression in the lungs were determined to explore potential changes induced by iron deficiency that might alter metal absorption. The pharmacokinetic curves for intratracheally instilled ^{54}Mn and ^{59}Fe were significantly different, suggesting that pulmonary uptake of the two metals involves different mechanisms. Intratracheally instilled iron-deficient rats had significantly higher blood ^{54}Mn levels, whereas blood ^{59}Fe levels were significantly reduced compared with controls. The same trend was observed when radioisotopes were delivered by intravenous injection, indicating that iron-deficient rats have altered blood clearance of manganese. In situ analysis revealed the presence of DMT1 transcripts in airway epithelium; however, mRNA levels did not change in iron deficiency. Although lung DMT1 levels and metal absorption did not appear to be influenced by iron deficiency, the differences in blood clearance of instilled manganese identified by this study support the idea that iron status can influence the potential toxicity of this metal.

divalent metal transporter 1; iron metabolism; manganese toxicity; lung metal absorption

NEUROTOXIC EFFECTS OF MANGANESE due to occupational airborne exposures are well documented. Workers exposed to high concentrations often display a Parkinson's-like disorder called manganism (24, 25, 31, 35). More recently, concern has been raised over the potential consequences of chronic low-level airborne exposures due to the introduction of methylcyclopentadienyl manganese tricarbonyl (MMT), a gasoline additive (3). Despite the importance of understanding the molecular basis for intoxication by airborne manganese, however, absorption of this metal from the lungs to the blood has yet to be fully explored.

Divalent metal transporter 1 (DMT1), a transporter that interacts with both iron and manganese (12, 21, 22), is expressed by airway epithelial cells (36) and could be involved in active uptake of both metals by the lungs. Two of the known DMT1 mRNA isoforms contain iron-responsive elements (IREs) and are therefore subject to potential regulation by iron response proteins (23). Iron deficiency is known to be an important modifier of manganese absorption in the gut (8, 9, 20, 26, 37), and DMT1 mRNA levels are dramatically upregulated in enterocytes of iron-deficient rats (22). Importantly, iron deficiency promotes the accumulation of manganese in the brain (9, 18). In particular, the globus pallidus is significantly affected (19), and this region of the brain is thought to be vulnerable to manganese-induced neurotoxicity (34).

To better characterize metal absorption from the lungs to the blood and test whether iron deficiency may modify this process, we compared the pharmacokinetics of pulmonary manganese and iron uptake by control (iron-replete) and iron-deficient rats. DMT1 mRNA levels in the lungs were also examined. The pharmacokinetic curves for intratracheally instilled ^{54}Mn and ^{59}Fe were significantly different, suggesting that pulmonary uptake of the two metals involves different mechanisms. DMT1 levels and lung metal absorption did not appear to be influenced by iron deficiency; however, significant differences in the clearance of instilled manganese were identified in iron-deficient rats, supporting the idea that iron status can influence the potential toxicity of this metal when absorbed by the lungs.

METHODS

Animal care and diets. Animal protocols for this study were approved by the Harvard Medical Area Animal Care and Use Committee of Harvard University. Male CD/Hsd rats (21 days old) were purchased from Harlan Sprague Dawley (Indianapolis, IN). Rats were maintained on a 12-h light/dark cycle and were given food and water ad libitum. To induce iron deficiency, rats were fed a low-iron diet containing 20–25 ppm Fe for 3 wk (Purina test diet no. 7444; PharmaServ, Framingham, MA). Age-matched control rats were fed a standard diet containing ~200 ppm Fe (Purina diet no. 5053). To confirm iron deficiency, heparinized blood samples were centrifuged at 3,000 *g* for 10 min to determine hematocrit values. After measurement of hematocrits, pharmacokinetic experiments were carried out as described below, and rats were humanely killed for collection of tissues. To further verify low-iron status of rats on an iron-deficient diet, non-heme iron content of liver and lung tissues was also determined using the method of Torrance and Bothwell (33).

Pharmacokinetic experiments. $^{54}MnCl_2$ and $^{59}FeCl_3$ were purchased from Perkin Elmer/NEN (Boston, MA). Stock ^{59}Fe was

Address for reprint requests and other correspondence: M. Wessling-Resnick, Dept. of Genetics and Complex Diseases, Harvard School of Public Health, 665 Huntington Ave., Boston, MA 02115 (E-mail: wessling@hsph.harvard.edu).

The costs of publication of this article were defrayed in part by the payment of page charges. The article must therefore be hereby marked "*advertisement*" in accordance with 18 U.S.C. Section 1734 solely to indicate this fact.

diluted 1:4,000 (vol/vol) in 10 mM sodium ascorbate. Radioisotopes were further diluted in sterile PBS (pH 7.4) before instillation or injection. To deliver radioisotope to the lungs, rats were anesthetized with vaporized halothane (Halocarbons Lab, North Augusta, SC) and intratracheally instilled with 1.5 ml of diluted radioisotope/kilogram of body weight (equivalent to 18 μCi ^{59}Fe/kg or 22.5 μCi ^{54}Mn/kg). Based on specific activity of radioisotopes, rats were given 0.9 μg of Fe/kg or 3.0 ng of Mn/kg. Briefly, rats were placed on a slanted platform, supported by an elastic band placed under the upper incisors. ^{54}Mn or ^{59}Fe was delivered to the lungs via a blunt 18-gauge needle inserted between the vocal chords and into the trachea. Transillumination of the larynx was provided by a microscope lamp shining on the neck (5). For intravenous injection of radioisotopes, rats were anesthetized with vaporized halothane, and 0.5 ml of diluted radioisotope/kilogram of body weight (18 μCi ^{59}Fe/kg or 22.5 μCi ^{54}Mn/kg) were injected into the penile vein. After instillation or injection of radioisotopes, rats were immediately placed in metabolic cages and supplied with food and water ad libitum. Blood samples were drawn from the tail artery at 5, 15, 30, 60, 120, and 240 min after instillation or injection. Four hours after administration of radioisotope, animals were anesthetized with vaporized halothane and killed by exsanguination, and tissues (lungs, brain, heart, spleen, kidney, skeletal muscle, liver, bone marrow, and gastrointestinal tract) and a final blood sample were collected. Radioactivity in organs and blood samples was measured in a gamma counter (Cobra Quantum, Packard Instruments). All tissue and blood samples were weighed, and radioactivity in tissues was calculated as % of instilled dose. For blood, skeletal muscle, and bone marrow, calculation of % instilled dose was based on estimation of tissue weight as a fraction of body weight (skeletal muscle, 45%; bone marrow, 3%; blood, 7%) (16).

In situ hybridization. After death, the tracheas of control and iron-deficient rats were cannulated with a blunt 18-gauge needle and syringe filled with OCT (optimum cutting temperature) compound (Sakura Finetek USA, Torrance, CA) prewarmed to 37°C. Lungs were filled with OCT, cut laterally into sections, mounted in OCT, snap-frozen in 2-methylbutane chilled on dry ice, and stored at −80°C. Ten-micrometer-thick sections were cut on a cryotome and stored at −20°C until processed. In situ hybridization was performed as described elsewhere (22). Briefly, digoxigenin-labeled sense and antisense cRNA probes were transcribed from a rat DMT1 cDNA fragment (bases 105–1788) flanked by T7 and SP6 promoter sites. Transcripts were shortened to an average length of 200–400 bp by alkali hydrolysis. Sections were incubated with sense or antisense probe (~200 ng/ml) in hybridization buffer (50% formamide, 5× SSC, 2% blocking reagent, 0.02% SDS, 0.1% *N*-laurylsarcosine). Hybridized probes were detected using anti-digoxigenin-alkaline phosphatase-coupled Fab fragments and bromo-4-chloro-3-indoxyl-phosphate and nitro blue tetrazolium as a substrate. Sections were incubated in substrate solution for 42 h, rinsed in TE buffer (10 mM Tris and 1 mM EDTA, pH 8.0), and mounted in 50% PBS/glycerol.

RT-PCR. After 3 wk on the diet as described above, rats were humanely killed. Lungs were excised and immediately submerged in RNA-Later (Ambion, Austin, TX). Duodena (~2 cm of small intestine proximal to stomach) were flushed with sterile PBS and then placed in RNA-Later. Tissues were stored in RNA-Later at −20°C until use. RNA was isolated from tissue with RNA-Bee (Tel-Test, Friendswood, TX) following the manufacturer's instructions. RNA was treated with DNase I (Promega, Madison, WI) to remove genomic DNA, extracted with phenol/chloroform/isoamyl alcohol (25:24:1) mixture, precipitated, resuspended in diethyl pyrocarbonate-treated water, and quantified by UV spectrophotometry. cDNA was synthesized from 2 μg of lung RNA or 0.5 μg of duodenum RNA in reactions containing 1× Moloney murine leukemia virus-reverse transcriptase (MMLV-RT) buffer, 0.5 mM dNTP mix, 25 μg/ml oligo(dT)15 primer, 5 mM $MgCl_2$, 10 mM dithiothreitol, 1 unit of RNasin, and 200 units of MMLV-RT enzyme (Promega). Amplification reactions were carried out with 2 μl of cDNA in 1× PCR buffer (10 mM Tris·HCl, pH 9.0, 50 mM KCl, 2.0 mM $MgCl_2$; Promega) with primer sets specific for the 3′-untranslated regions of DMT1-IRE and DMT1-non-IRE isoforms (IRE forward: 5′-TCCTGCTGAGC-GAAGATACC-3′; IRE reverse: 5′-AGACCTCCCCTGACAAAA-3′; non-IRE forward: 5′-GAACACTTTCTCTAAGCCCT-3′; non-IRE reverse: 5′-CTTACCCAAACTGGCACG-3′). Amplification reactions were carried out for 28, 32, and 36 cycles. Fifteen microliters of each reaction was separated on an agarose gel containing ethidium bromide, and band intensity was quantified with QuantityOne software (Bio-Rad, Hercules, CA). Linear equations were calculated for each set of three reactions and used to determine the cycle number at which the product accumulated to a threshold level. Amplification reactions were carried out with primers for β-actin as described elsewhere (1). PCR products were quantified after 18, 21, and 24 amplification cycles, and cycle number at the threshold level was calculated as described above. Fold induction of DMT1 isoforms was normalized to β-actin expression.

Statistical analysis. All values are means ± SE. Comparisons of control and iron-deficient groups in the pharmacokinetic experiments (Figs. 1 and 2) and deposition of radioisotopes in blood and tissues (Tables 2 and 3; Fig. 3) were evaluated by multivariate analysis of variance (MANOVA) using the general linear model procedure (SAS statistical analysis software; SAS Institute, Cary, NC). *P* values for radioisotope absoprtion by individual organs were determined by

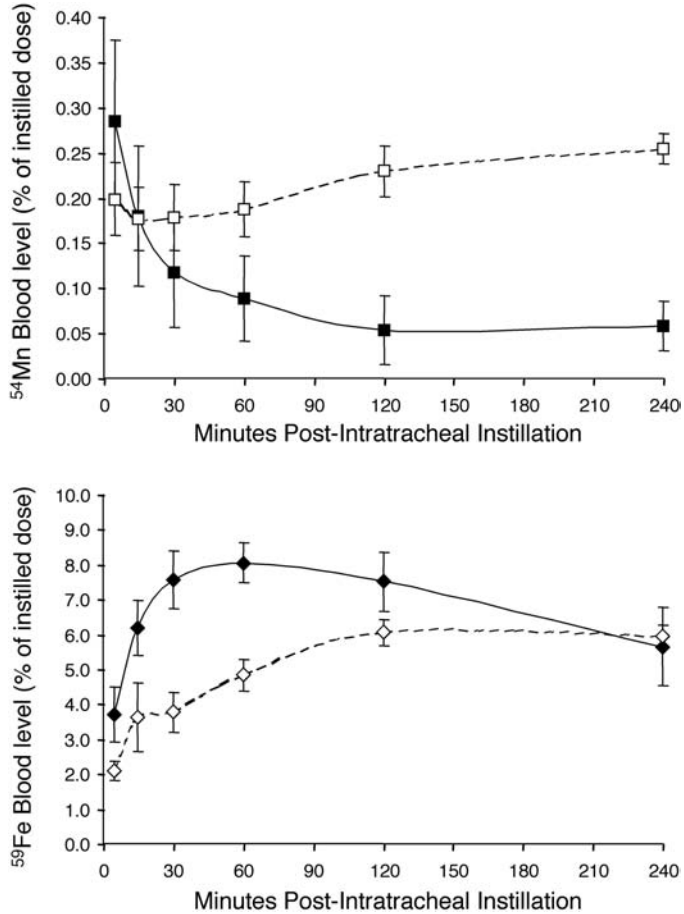

Fig. 1. Vascular kinetics of intratracheally instilled ^{54}Mn and ^{59}Fe. Control (filled symbols) and iron-deficient (open symbols) rats were intratracheally instilled with 22.5 μCi $^{54}MnCl_2$/kg body wt (*top*) or 18 μCi $^{59}FeCl_3$/kg body wt (*bottom*). Blood was drawn by tail artery puncture at 5, 15, 30, 60, 120, and 240 min after instillation. Radioactivity in blood is expressed as % instilled dose and is plotted as a function of time ($n = 7$ for ^{54}Mn and $n = 5$ for ^{59}Fe groups).

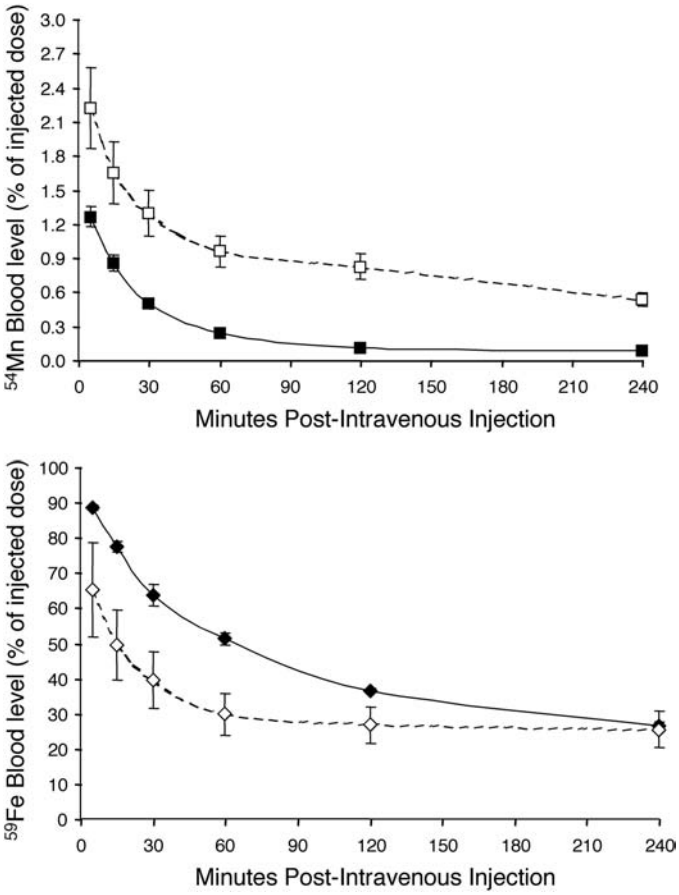

Fig. 2. Vascular kinetics of intravenously injected ^{54}Mn and ^{59}Fe. Control (filled symbols) and iron-deficient (open symbols) rats were intravenously injected in the penile vein with 22.5 μCi $^{54}MnCl_2$/kg body wt (*top*) or 18 μCi $^{59}FeCl_3$/kg body wt (*bottom*). Radioactivity is expressed as % of injected dose remaining in blood drawn from the tail artery and is plotted as a function of time ($n = 5$ for ^{54}Mn and $n = 4$ for ^{59}Fe groups).

F-test, using all organ radioisotope values as responses. Characteristics of control and iron-deficient rats (Table 1) and comparisons of DMT1 expression by RT-PCR (Fig. 4) were evaluated by Student's unpaired *t*-test. All statistical significance was based on an alpha level of 0.05.

RESULTS

Characteristics of iron-deficient rats. After 3 wk on a low-iron diet, rats had significantly reduced hematocrit and body weights (Table 1). Non-heme iron levels in the livers of control and iron-deficient groups were also significantly different. Although a trend toward lower non-heme iron levels in iron-deficient lung tissue was observed, statistical significance was not achieved.

Pharmacokinetics of intratracheally instilled ^{54}Mn and ^{59}Fe. To compare pharmacokinetics of pulmonary manganese absorption in iron-deficient and iron-replete rats, ^{54}Mn was instilled intratracheally, and blood radioisotope levels were determined in samples drawn at intervals from 5 min to 4 h after administration of isotope (Fig. 1). For control (iron-replete) rats, a rapid initial drop in blood ^{54}Mn levels was observed in the first 30 min postinstillation, after which time radioisotope levels remained relatively stable at ~0.05% of the total dose up to 4 h. In contrast, in the iron-deficient group, the initial decrease in ^{54}Mn levels was not as marked, and there was a gradual increase in ^{54}Mn blood levels over time that was significantly higher than controls (MANOVA, $P < 0.05$). At 4 h postinstillation, ^{54}Mn levels in blood were almost fourfold higher in iron-deficient rats compared with controls. Furthermore, the rate of change in ^{54}Mn levels over time was significantly different for the control and iron-deficient groups (MANOVA, $P < 0.05$).

Similar experiments were performed to compare the pharmacokinetics of ^{59}Fe uptake from the lungs to the blood. The time course for intratracheally instilled ^{59}Fe was quite different from that of ^{54}Mn (Fig. 1). In the control group, ^{59}Fe levels increased rapidly in the first 30 min after instillation, achieving a maximal plateau at ~8% of the instilled dose between 30 and 60 min. By 2 h postinstillation, ^{59}Fe blood levels began to decline and decreased to ~5.5% at 4 h. In iron-deficient rats, there was a more gradual increase in blood ^{59}Fe levels, with maximal circulating levels of ~6% of instilled dose observed 2 h postinstillation and remaining constant over the time course studied. In contrast to the pharmacokinetics of ^{54}Mn absorption, blood ^{59}Fe levels were significantly lower in iron-deficient rats (MANOVA, $P < 0.05$). The rates of change in ^{59}Fe levels for each group and the variation over time were also significantly different (MANOVA, $P < 0.05$).

Pharmacokinetics of intravenously injected ^{54}Mn and ^{59}Fe. To assess the contribution of blood clearance in the pharmacokinetics of lung ^{54}Mn and ^{59}Fe absorption, time course experiments were performed to evaluate ^{54}Mn or ^{59}Fe levels after intravenous injection (Fig. 2). Blood ^{54}Mn levels dropped rapidly such that at 5 min after injection, only 1–2% of isotope remained in the circulation. These data are comparable to results previously reported for human (13) and animal (9) studies. The rates of clearance were not significantly different between the control and iron-deficient groups, an observation also consistent with a previous report by Chua and Morgan (9). However, in contrast to the latter study (9), the iron-deficient rats in our study had significantly higher ^{54}Mn blood levels (MANOVA, $P < 0.05$). The opposite trend was observed for rats injected with ^{59}Fe. Iron-deficient rats had significantly

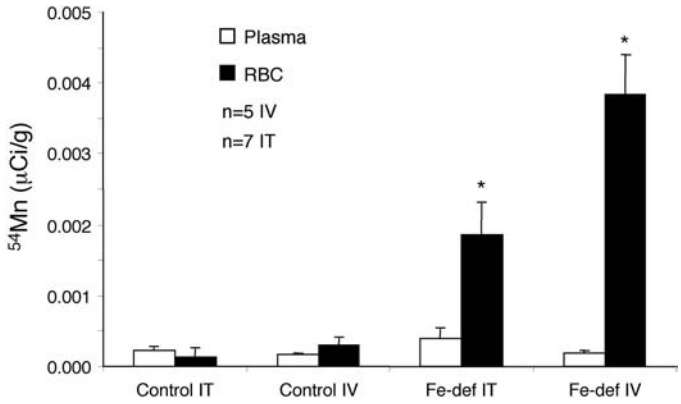

Fig. 3. Distribution of ^{54}Mn in plasma and cellular fractions of blood. Control and iron-deficient (Fe-def) rats were intratracheally instilled (IT) ($n = 7$) or intravenously injected (IV) ($n = 5$) with ^{54}Mn. Isotope levels (μCi/g) were determined by gamma counting plasma (open bars) and cellular fractions (solid bars) of blood samples collected 4 h after administration (*$P < 0.005$). RBC, red blood cells.

Table 1. *Characteristics of 6-wk-old rats*

	% Hematocrit	Body Weight, g	Liver Non-Heme Iron†	Lung Non-Heme Iron†
Control	43.4±0.8 (n=30)	217.3±9.2 (n=30)	67.91±5.87 (n=4)	16.7±1.28 (n=3)
Fe-deficient	25.1±0.6*(n=31)	144.4±6.4*(n=31)	9.57±0.83*(n=6)	14.5±0.80 (n=5)

Values are means ± SE. *$P < 0.005$; †expressed as μg of Fe/g wet tissue.

lower ^{59}Fe blood levels, and the rate of clearance from the circulation was greater in the iron-deficient group than in controls (MANOVA, $P < 0.05$). These results are concordant with data obtained when ^{59}Fe injected intravenously was complexed to transferrin (9).

Absorption of ^{54}Mn and ^{59}Fe by tissues. The distribution of radioisotopes 4 h postinstillation was determined for the organs listed in Tables 2 and 3. Uptake of ^{54}Mn and ^{59}Fe by peripheral tissues was significantly different and was affected by both iron status and route of administration. In iron-deficient rats instilled intratracheally, a marked accumulation of ^{54}Mn in the small intestine (~12% of instilled dose) was noted. Because a major excretory route for manganese is through biliary secretion (4), and intestinal absorption of this metal is upregulated by iron deficiency (32), this effect most likely reflects duodenal reabsorption. In humans, Mena et al. (26) observed a decline in ^{54}Mn radioactivity in the lungs (measured by exterior regional counting with a scintillation detector) with a concurrent increase in the epigastric region, consistent with the results of our study. Significantly less ^{54}Mn accumulated in liver, kidney, and skeletal muscle in iron-deficient rats compared with controls. In contrast, iron-deficient rats instilled with ^{59}Fe accumulated more isotope in the liver and less in the small intestine compared with controls.

The majority of instilled radioisotope remained in the lungs in all groups, and although more ^{54}Mn and ^{59}Fe remained in the lungs in iron-deficient rats, this increase was not statistically significant. These data indicate that pulmonary uptake of iron and manganese is not significantly altered by iron deficiency. Generally, at 4 h, more ^{59}Fe remained in the lungs (75–80% of dose) than did ^{54}Mn (61–65% of dose), suggesting that the latter metal is absorbed more rapidly.

In rats given ^{54}Mn by intravenous injection, significantly more ^{54}Mn accumulated in the brain in the iron-deficient group (Table 3). These data agree with previous studies that have shown brain manganese levels are higher in iron-deficient rats (37). We also observed significant deposition in the small intestine, similar to the increased levels seen in iron-deficient rats instilled intratracheally with ^{54}Mn, suggesting that, in both cases, iron-deficient rats effect greater biliary excretion of manganese with reabsorption of the metal.

The tissue distribution of ^{59}Fe injected intravenously into control and iron-deficient animals was not remarkably different. Similar to the instilled group, the liver of iron-deficient rats accumulated significantly more isotope. One major difference noted between the routes of administration was that ^{59}Fe levels in the spleen of injected rats were diminished in the iron-deficient group compared with controls.

Radioisotope distribution in plasma and cellular fractions of blood. The distribution of ^{54}Mn between plasma and red blood cells was measured 4 h postinstillation or postinjection. A substantial increase in radioisotope was observed in red blood cells of iron-deficient rats compared with controls regardless of the route of administration (Fig. 3).

DMT1 expression in the lungs. To determine whether lung DMT1 mRNA expression responds to iron deficiency, in situ hybridization was performed (Fig. 4*A*). DMT1 mRNA was detected in airway epithelial cells, but no obvious change was observed in the lungs of iron-deficient rats. DMT1 mRNA was faintly detected in alveolae. Because the probe used for in situ hybridization detected both the IRE and non-IRE isoforms of DMT1, additional semiquantitative RT-PCR experiments were performed to assess the expression level of the individual isoforms (Fig. 4*B*). We observed an ~1-fold increase in the non-IRE isoform and an ~0.8-fold increase in the IRE isoform in lung tissue from iron-deficient rats; however, neither change was statistically significant. In contrast, a threefold increase in the IRE isoform with a more modest increase in the non-IRE isoform in duodenum from the same group of animals was observed (Fig. 4*B*).

DISCUSSION

This study was undertaken to characterize metal absorption from the lungs to the blood and to test whether iron deficiency may modify this process. The pharmacokinetic curves for ^{54}Mn administered by intratracheal instillation or intravenous injection demonstrate that blood manganese levels are higher in iron-deficient rats regardless of the route of administration. Four hours after instillation or injection of ^{54}Mn, blood levels were ~3.5- to 4-fold higher in iron-deficient rats. Because the proportion of instilled isotope remaining in the lungs was not significantly different in iron-deficient rats, we can conclude that the rate of manganese absorption from the lungs into the circulation is not significantly increased by iron deficiency but that clearance of instilled manganese from circulation is reduced. The pharmacokinetic curves for ^{59}Fe absorption were markedly different from results obtained with ^{54}Mn. Accumulation of instilled isotope in circulation was delayed, with a more gradual increase observed in blood levels of iron-deficient rats. Although this delay might be attributable to a modifying effect of iron deficiency on lung iron absorption, blood clearance of ^{59}Fe injected intravenously was more rapid in these animals. Moreover, the amount of instilled isotope remaining in the lungs 4 h postinstillation was not significantly different between the two groups. Thus iron deficiency also does not appear to significantly enhance absorption of instilled ^{59}Fe by the lungs. In contrast to instilled manganese, however, instilled iron is cleared more rapidly from circulation in iron-deficient rats.

Whether injected or instilled, ^{54}Mn accumulated in the cellular fraction of blood samples from iron-deficient animals. Manganese is predominantly found in erythrocytes (29), and high manganese levels in red blood cells from iron-deficient human subjects have been previously observed (26). There is

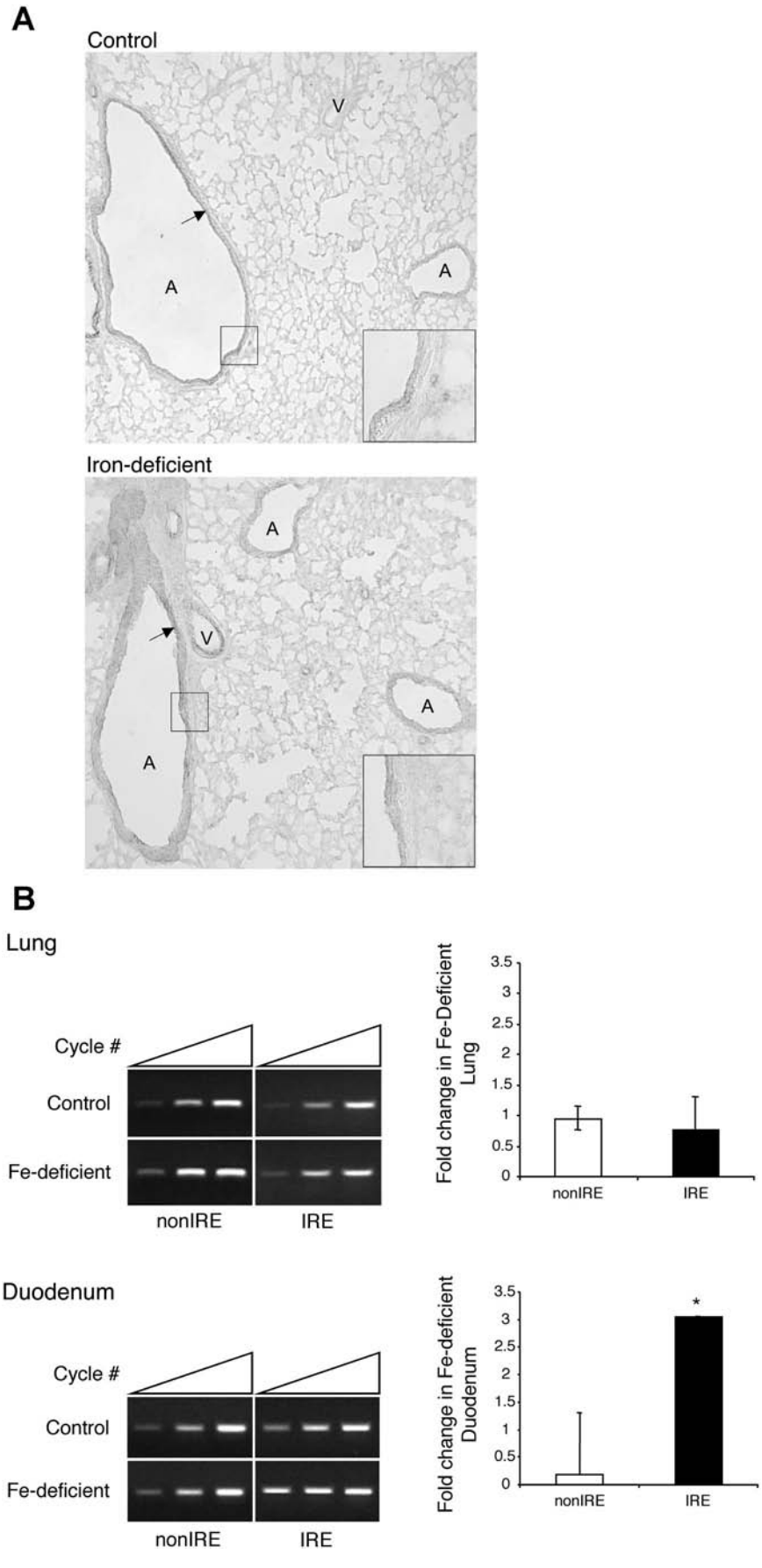

Fig. 4. Divalent metal transporter 1 (DMT1) mRNA expression in lung. *A*: in situ hybridization for DMT1. DMT1 mRNA was detected in airway epithelial cells with a probe recognizing both +iron-responsive element (+IRE) and −IRE isoforms (arrows) as described in METHODS. Shown are representative results comparing the staining profile and intensity for control (*top*) and iron-deficient (*bottom*) rats. A, airway; V, blood vessel. *Insets*: intense staining of airway epithelial cells in control and iron-deficient rats. *B*: RT-PCR with isoform-specific primers for DMT1. To determine whether isoform-specific changes in DMT1 mRNA levels could be detected in iron-deficient animals, semiquantitative RT-PCR reactions were carried out as described in METHODS using total RNA isolated from lungs (*top*) and duodenum (*bottom*) for cDNA synthesis. The fold induction of DMT1 IRE and non-IRE isoforms was normalized to β-actin expression ($*P < 0.05$).

Table 2. *Distribution of ^{54}Mn and ^{59}Fe in tissues 4 h after intratracheal instillation of $^{54}MnCl_2$ or $^{59}FeCl_3$*

	^{54}Mn		^{59}Fe	
	Control	Fe deficient	Control	Fe deficient
Brain	0.065±0.004	0.056±0.006	0.049±0.012	0.081±0.029
Liver	7.932±0.432	6.169±0.272*	3.097±0.179	4.759±0.570*
Spleen	0.221±0.013	0.214±0.034	0.580±0.305	0.756±0.216
Lungs	60.661±1.674	64.723±1.481	75.459±3.607	80.466±2.378
Kidney	2.410±0.138	1.423±0.069*	0.324±0.029	0.243±0.046
Heart	0.328±0.024	0.360±0.015	0.145±0.031	0.166±0.032
Bone marrow	0.699±0.069	0.732±0.056	2.204±0.232	2.294±0.378
Skeletal muscle	4.043±0.303	3.019±0.222*	2.852±0.683	3.817±2.011
Stomach	1.261±0.386	1.447±0.472	0.834±0.244	2.026±0.501
Small intestine	4.911±0.718	12.273±1.330*	4.462±0.632	1.631±0.222*
Large intestine	3.557±0.730	1.136±0.163*	2.177±1.729	0.339±0.134
Total recovered	86.154±0.609	91.811±1.328	97.882±1.400	102.531±3.974

Values are means ± SE. Radioactivity is expressed as % of total instilled dose for each rat. Total % dose recovered is the sum of radioactivity in organs shown above plus urine, feces, and blood at 4 h. For $^{54}MnCl_2$, $n = 7$; $^{59}FeCl_3$, $n = 5$; multivariate ANOVA, $*P < 0.05$.

evidence that manganese can incorporate into porphyrin (15), and it is conceivable that this process occurs more readily in the anemic state. We do not yet know whether manganese absorbed by the lungs enters circulation as Mn(II) or Mn(III). Trivalent manganese can bind to transferrin, and this serum protein is believed to be the major carrier for circulating manganese (2). Transferrin levels are enhanced by iron deficiency, and this effect is most likely responsible for the increased clearance of ^{59}Fe from the blood that we observed. Thus the major difference in the partitioning of the two isotopes between plasma and cellular fractions of blood in iron-deficient rats suggests that unique pathways for manganese uptake and/or retention may exist. For example, in addition to the uptake of transferrin-bound manganese, high- and low-affinity transport of Mn(II) by reticulocytes and erythrocytes has been reported (10).

As part of our investigation, we considered whether DMT1 might play a role in pulmonary metal uptake. This transporter has been shown to be directly involved in both iron and manganese transport (11, 12, 21, 22), and its activity is thought to be regulated by iron deficiency (7, 22, 23). In situ hybridization shows that DMT1 mRNA is present in airway epithelia; however, the pattern of DMT1 expression did not change in lungs of iron-deficient rats. Semiquantitative RT-PCR shows that neither the IRE nor non-IRE DMT1 isoforms present in lung tissue are altered by iron deficiency. The lack of iron-responsive DMT1 regulation most likely reflects the fact that lung non-heme iron content was not significantly different between control and iron-deficient rats. These data are generally compatible with the fact that iron deficiency does not enhance pulmonary metal uptake, but that does not exclude a role for DMT1 in lung metal absorption. Further work is necessary to define the molecular basis of iron and manganese uptake by the lungs. On the basis of their pharmacokinetic profiles, absorption of ^{59}Fe and ^{54}Mn appears to be mediated through different mechanisms, although DMT1 could potentially play a role in both pathways. Although we were unsuccessful at detecting DMT1 protein expression in the lungs using commercially available antisera, others have reported that the non-IRE DMT1 isoform is upregulated in the lung epithelium upon exposure to ferric ammonium citrate (36). It will therefore be of great interest to study potential changes in the pharmacokinetics of metal uptake by the lungs under similar conditions.

In community-based studies, neurological effects resulting from airborne manganese exposure vary considerably on an individual basis, falling into what Mergler et al. (28) term a "continuum of dysfunction." Iron status is one variable that may determine susceptibility to manganese poisoning. Increased absorption and retention of manganese in the brains of

Table 3. *Distribution of ^{54}Mn and ^{59}Fe in tissues 4 h after intravenous injection of $^{54}MnCl_2$ or $^{59}FeCl_3$*

	^{54}Mn		^{59}Fe	
	Control	Fe deficient	Control	Fe deficient
Brain	0.209±0.015	0.395±0.044*	0.132±0.015	0.204±0.035
Liver	21.846±1.756	20.976±1.980	12.577±0.270	19.369±1.732*
Spleen	0.743±0.033	0.680±0.059	7.405±0.889	3.076±1.130*
Lungs	1.023±0.092	2.947±1.154	0.705±0.068	0.718±0.115
Kidney	8.023±0.428	7.384±0.965	1.070±0.028	0.976±0.220
Heart	1.265±0.088	2.716±0.729	0.492±0.011	0.609±0.138
Bone marrow	2.319±0.093	3.593±0.660	9.454±0.821	8.979±1.082
Skeletal muscle	12.733±0.978	12.109±0.745	11.068±1.325	15.379±6.437
Stomach	1.179±0.041	1.922±0.259*	0.668±0.128	0.635±0.163
Small intestine	19.046±0.761	28.662±1.523*	4.024±0.278	3.874±0.510
Large intestine	5.552±0.978	6.565±0.570	1.210±0.098	0.810±0.153
Total recovered	74.033±0.628	88.922±5.577	75.636±1.894	80.246±3.404

Values are means ± SE. Radioactivity is expressed as % of total injected dose for each rat. Total % dose recovered is the sum of radioactivity in organs shown above plus urine, feces, and blood at 4 h. For $^{54}MnCl_2$, $n = 7$; $^{59}FeCl_3$, $n = 5$; multivariate ANOVA, $*P < 0.05$.

iron-deficient rats has been well documented (8, 9, 18, 19, 27, 37). Whereas excess manganese absorbed by the gut is subject to hepatobiliary clearance due to portal circulation (6, 30), manganese entering the blood stream via the lungs can first reach the brain and other peripheral tissue. We observed that iron deficiency promoted significant changes in the blood clearance of instilled manganese, resulting in greater retention of the metal in circulation. In human subjects, elevated blood manganese levels correlate with lower serum ferritin (20), lower dietary intake of non-heme iron (14), and lower levels of circulating soluble transferrin receptor (17). We observed that blood manganese levels remained elevated in iron-deficient rats due to accumulation of ^{54}Mn in the cellular fraction. We speculate that gradual release of manganese from senescing red blood cells during iron deficiency could prolong and/or modify the consequences of exposure to this toxic metal. Chronic exposure to high levels of manganese can lead to manganism, an irreversible neurological disorder (24, 25, 31, 35). Because of the introduction of manganese into gasoline in the anti-knock agent MMT, there has been heightened concern over the effects of low-level chronic exposure to airborne manganese (3). Our study indicates that iron status is one variable that should be further examined to fully evaluate the risk of neurotoxicity from environmental manganese.

ACKNOWLEDGMENTS

We thank Dr. Khristy Thompson for carefully reading the manuscript and for helpful experimental advice.

GRANTS

This work was supported by National Institute of Diabetes and Digestive and Kidney Diseases Grant DK-60528.

REFERENCES

1. **Abe T, Sato M, and Tamai M.** Dedifferentiation of the retinal pigment epithelium compared to the proliferative membranes of proliferative vitreoretinopathy. *Curr Eye Res* 17: 1103–1109, 1998.
2. **Aschner M and Aschner JL.** Manganese transport across the blood-brain barrier: relationship to iron homeostasis. *Brain Res Bull* 24: 857–860, 1990.
3. **Aschner M.** Manganese: brain transport and emerging research needs. *Environ Health Perspect* 108: 429–432, 2000.
4. **Bertinchamps AJ, Miller ST, and Cotzias GC.** Interdependence of routes excreting manganese. *Am J Physiol* 211: 217–224, 1966.
5. **Brain JD, Knudson DE, Sorokin SP, and Davis MA.** Pulmonary distribution of particles given by intratracheal instillation or by aerosol inhalation. *Environ Res* 11: 13–33, 1976.
6. **Britton AA and Cotzias GC.** Dependence of manganese turnover on intake. *Am J Physiol* 211: 203–206, 1966.
7. **Canonne-Hergaux F, Gruenheid S, Ponka P, and Gros P.** Cellular and subcellular localization of the Nramp2 iron transporter in the intestinal brush border and regulation by dietary iron. *Blood* 93: 4406–4417, 1999.
8. **Chandra SV and Shukla GS.** Role of iron deficiency in inducing susceptibility to manganese toxicity. *Arch Toxicol* 35: 319–323, 1976.
9. **Chua AC and Morgan EH.** Effects of iron deficiency and iron overload on manganese uptake and deposition in the brain and other organs of the rat. *Biol Trace Elem Res* 55: 39–54, 1996.
10. **Chua AC, Stonell LM, Savigni DL, and Morgan EH.** Mechanisms of manganese transport in rabbit erythroid cells. *J Physiol* 493: 99–112, 1996.
11. **Chua AC and Morgan EH.** Manganese metabolism is impaired in the Belgrade laboratory rat. *J Comp Physiol* 167: 361–369, 1997.
12. **Conrad ME, Umbreit JN, Moore EG, Hainsworth LN, Porubcin M, Simovich MJ, Nakada MT, Dolan K, and Garrick MD.** Separate pathways for cellular uptake of ferric and ferrous iron. *Am J Physiol Gastrointest Liver Physiol* 279: G767–G774, 2000.
13. **Cotzias GC, Horiuchi K, Fuenzalida S, and Mena I.** Chronic manganese poisoning. Clearance of tissue manganese concentrations with persistence of the neurological picture. *Neurology* 18: 376–382, 1968.
14. **Davis CD, Malecki EA, and Greger JL.** Interactions among dietary manganese, heme iron, and nonheme iron in women. *Am J Clin Nutr* 56: 926–932, 1992.
15. **Diez-Ewald M, Weintraub LR, and Crosby WH.** Interrelationship of iron and manganese metabolism. *Proc Soc Exp Biol Med* 129: 448–451, 1968.
16. **Diluzio NR and Zilversmit DB.** Influence of exogenous proteins on blood clearance and tissue distribution of colloidal gold. *Am J Physiol* 180: 563–565, 1955.
17. **Ellingsen DG, Haug E, Ulvik RJ, and Thomassen Y.** Iron status in manganese alloy production workers. *J Appl Toxicol* 23: 239–247, 2003.
18. **Erikson KM, Shihabi ZK, Aschner JL, and Aschner M.** Manganese accumulates in iron-deficient rat brain regions in a heterogeneous fashion and is associated with neurochemical alterations. *Biol Trace Elem Res* 87: 143–156, 2002.
19. **Erikson KM, Syversen T, Steinnes E, and Aschner M.** Globus pallidus: a target brain region for divalent metal accumulation associated with dietary iron deficiency. *J Nutr Biochem* 15: 335–341, 2004.
20. **Finley JW.** Manganese absorption and retention by young women is associated with serum ferritin concentration. *Am J Clin Nutr* 70: 37–43, 1999.
21. **Forbes JR and Gros P.** Iron, manganese, and cobalt transport by Nramp1 (Slc11a1) and Nramp2 (Slc11a2) expressed at the plasma membrane. *Blood* 102: 1884–1892, 2003.
22. **Gunshin H, Mackenzie B, Berger UV, Gunshin Y, Romero MF, Boron WF, Nussberger S, Gollan JL, and Hediger MA.** Cloning and characterization of a mammalian proton-coupled metal-ion transporter. *Nature* 388: 482–488, 1997.
23. **Gunshin H, Allerson CR, Polycarpou-Schwarz M, Rofts A, Rogers JT, Kishi F, Hentze MW, Rouault TA, Andrews NC, and Hediger MA.** Iron-dependent regulation of the divalent metal ion transporter. *FEBS Lett* 509: 309–316, 2001.
24. **Korczynski RE.** Occupational health concerns in the welding industry. *Appl Occup Environ Hyg* 15: 936–945, 2000.
25. **Lucchini R, Bergamaschi E, Smargiassi A, Festa D, and Apostoli P.** Motor function, olfactory threshold, and hematological indices in manganese-exposed ferroalloy workers. *Environ Res* 73: 175–180, 1997.
26. **Mena I, Horiuchi K, Burke K, and Cotzias GC.** Chronic manganese poisoning. Individual susceptibility and absorption of iron. *Neurology* 19: 1000–1006, 1969.
27. **Mena I.** The role of manganese in human disease. *Ann Clin Lab Sci* 4: 487–491, 1974.
28. **Mergler D, Baldwin M, Belanger S, Larribe F, Beuter A, Bowler R, Panisset M, Edwards R, de Geoffroy A, Sassine MP, and Hudnell K.** Manganese neurotoxicity, a continuum of dysfunction: results from a community based study. *Neurotoxicology* 20: 327–342, 1999.
29. **Milne DB, Sims RL, and Ralston NV.** Manganese content of the cellular components of blood. *Clin Chem* 36: 450–452, 1990.
30. **Papavasiliou PS, Miller ST, and Cotzias GC.** Role of liver in regulating distribution and excretion of manganese. *Am J Physiol* 211: 211–216, 1966.
31. **Roels H, Lauwerys R, Buchet JP, Genet P, Sarhan MJ, Hanotiau I, de Fays M, Bernard A, and Stanescu D.** Epidemiological survey among workers exposed to manganese: effects on lung, central nervous system, and some biological indices. *Am J Ind Med* 11: 307–327, 1987.
32. **Thomson AB, Olatunbosun D, and Valverg LS.** Interrelation of intestinal transport system for manganese and iron. *J Lab Clin Med* 78: 642–655, 1971.
33. **Torrance JD and Bothwell TH.** A simple technique for measuring storage iron concentrations in formalinised liver samples. *S Afr J Med Sci* 33: 9–11, 1968.
34. **Verity MA.** Manganese neurotoxicity: a mechanistic hypothesis. *Neurotoxicology* 20: 489–497, 1999.
35. **Wang JD, Huang CC, Hwang YH, Chiang JR, Lin JM, and Chen JS.** Manganese induced parkinsonism: an outbreak due to an unrepaired ventilation control system in a ferromanganese smelter. *Br J Ind Med* 46: 856–859, 1989.
36. **Wang X, Ghio AJ, Yang F, Dolan KG, Garrick MD, and Piantadosi CA.** Iron uptake and Nramp2/DMT1/DCT1 in human bronchial epithelial cells. *Am J Physiol Lung Cell Mol Physiol* 282: L987–L995, 2002.
37. **Yokoi K, Kimura M, and Itokawa Y.** Effect of dietary iron deficiency on mineral levels in tissues of rats. *Biol Trace Elem Res* 29: 257–265, 1991.